Journal of Athletic Training 2012;47(5):489–497
doi: 10.4085/1062-6050-47.4.06

www.nata.org/journal-of-athletic-training

original research

Biomechanics of Sports-Induced Axial-Compression Injuries of the Neck

Paul C. Ivancic, PhD

Department of Orthopaedics and Rehabilitation, Yale University School of Medicine, New Haven, CT

Context: Head-first sports-induced impacts cause cervical fractures and dislocations and spinal cord lesions. In previous biomechanical studies, researchers have vertically dropped human cadavers, head-neck specimens, or surrogate models in inverted postures.

Objective: To develop a cadaveric neck model to simulate horizontally aligned, head-first impacts with a straightened neck and to use the model to investigate biomechanical responses and failure mechanisms.

Design: Descriptive laboratory study.

Setting: Biomechanics research laboratory.

Patients or Other Participants: Five human cadaveric cervical spine specimens.

Intervention(s): The model consisted of the neck specimen mounted horizontally to a torso-equivalent mass on a sled and carrying a surrogate head. Head-first impacts were simulated at 4.1 m/s into a padded, deformable barrier.

Main Outcome Measure(s): Time-history responses were determined for head and neck loads, accelerations, and motions. Average occurrence times of the compression force peaks at the impact barrier, occipital condyles, and neck were compared.

Results: The first local compression force peaks at the impact barrier (3070.0 ± 168.0 N at 18.8 milliseconds), occipital condyles (2868.1 ± 732.4 N at 19.6 milliseconds), and neck (2884.6 ± 910.7 N at 25.0 milliseconds) occurred earlier than all global compression peaks, which reached 7531.6 N in the neck at 46.6 milliseconds ($P < .001$). Average peak head motions relative to the torso were 6.0 cm in compression, 2.4 cm in posterior shear, and 6.4° in flexion. Neck compression fractures included occipital condyle, atlas, odontoid, and subaxial comminuted burst and facet fractures.

Conclusions: Neck injuries due to excessive axial compression occurred within 20 milliseconds of impact and were caused by abrupt deceleration of the head and continued forward torso momentum before simultaneous rebound of the head and torso. Improved understanding of neck injury mechanisms during sports-induced impacts will increase clinical awareness and immediate care and ultimately lead to improved protective equipment, reducing the frequency and severity of neck injuries and their associated societal costs.

Key Words: head-first impacts, cervical spine, injury mechanisms

Key Points

- A cadaveric neck model was developed to simulate horizontally aligned, head-first impacts with a straightened neck and used to investigate the biomechanical responses and failure mechanisms.
- The first local compression force peaks at the impact barrier, occipital condyles, and neck occurred earlier than all global compression peaks.
- Injuries included occipital condyle, atlas, odontoid, and subaxial comminuted burst and facet fractures.
- Neck injuries due to excessive axial compression occurred within 20 milliseconds of impact and were caused by abrupt deceleration of the head and continued forward torso momentum before simultaneous rebound of the head and torso.

Axial compression due to head-first impact is the predominant mechanism that causes severe neck injuries during sports, including football, rugby, hockey, diving, wrestling, gymnastics, trampolining, and equestrian sports.[1,2] Injuries include complete or incomplete spinal cord lesions, fractures, and dislocations and even death. Compression injuries include occipital condyle, atlas, and odontoid fractures at the upper cervical spine and comminuted burst, teardrop, and facet fractures at the middle and lower cervical spine. Most neck fractures occur at the lower cervical spine (C5 through C7), followed by the upper cervical spine (C1 and C2).[3] More than half of all spinal cord injuries occur in the cervical spine, and they are associated with greater morbidity than cord injuries in the thoracolumbar spine.[4] Estimated lifetime costs of caring for a patient with a spinal cord injury are between $1 million and $4 million.[5]

Rule changes in US football and improved training techniques have led to reduction, but not complete elimination, of severe neck injuries caused by spear tacking.[1] *Spear tackling* consists of flexing the neck, which causes straightening of the normal cervical lordosis, and striking the opponent with the top of the helmet. The head rapidly decelerates while the fragile neck is compressed traumatically between the head and oncoming torso. Despite rule changes and an overall decrease in catastrophic neck injuries, spearing and improper tackling techniques commonly occur.[6]

Mechanisms of neck injury due to simulated head-first impacts have been investigated using cadaveric,[7–12] surrogate,[13] and mathematical models.[14,15] Vertical drop tests of

human cadavers or head-neck specimens in inverted postures have demonstrated that the cervical spine buckles and fails due to axial compression caused by abrupt stoppage of the head and continued torso momentum. The osseous cervical spine is crushed between the head and oncoming torso. Researchers[10] have demonstrated that head constraint or pocketing of the head into a padded surface might increase the risk of neck injury compared with allowing the head and neck to flex or extend and move out of the path of the oncoming torso. Yoganandan et al[8] found greater head compressive loads and more neck injuries due to inverted drop tests in cadavers restrained with simulated muscle forces than unrestrained cadavers experienced. Head flexion or extension allows the neck muscles, ligaments, and discs to absorb some of the impact energy, thereby reducing the risk of neck fracture. The vertical drop tests of human cadavers have been successful in reproducing clinically relevant neck fractures, dislocations, and ligamentous and disc ruptures.[7–12]

The most comprehensive series of vertical drop tests using human head-neck specimens was performed by Nightingale et al.[7,9,10] The T1 vertebra was mounted rigidly to a load cell attached to a 16-kg mass on vertically oriented linear bearings. Neutral head and lordotic cervical spine postures were maintained before impact. Peak impact force ranged from 1.8 to 11.6 kN, and impact velocity was 3.2 m/s. High-speed camera recording of the experiments enabled visualization of neck-buckling patterns. They studied the effects of variables on neck injuries, including impact surface (high-friction padded surface or low-friction rigid surface) and impact surface angle (causing impacts posterior to, anterior to, or at the vertex of the head). Neck-buckling and failure patterns depended on the experimental condition and included first-order and higher-order buckling modes. The high-friction, padded surface caused greater neck injuries than the low-friction rigid surface. The greatest risk of neck injury occurred when the impact surface was oriented perpendicular to the cervical spine.

In contrast to the previous biomechanical experiments, most real-life head-first impacts occur to athletes when moving parallel or oblique to the ground, causing horizontally aligned neck compression.[16] Examples include athletes spear tackling in football or being checked head first into the boards in hockey. An inverted posture during vertical drop tests without simulated musculature causes neck tension immediately before impact; however, muscle bracing induces neck compression in real-life head-first impacts. Biomechanical neck responses and failure patterns during real-life head-first sports impacts might differ from those reported in the previous biomechanical studies. Therefore, the purpose of the present study was to develop a cadaveric neck model to simulate horizontally aligned head-first impacts with a straightened neck and to use the model to investigate biomechanical responses and failure mechanisms.

METHODS

Human Cadaver Neck Model With Surrogate Head

I prepared 5 fresh-frozen human osteoligamentous cervical spine specimens (2 men, 3 women; age = 86.8 ± 4.9 years). The specimens included occiput through C5 (specimens 2 and 3) or C6 (specimens 1, 4, and 5). Apart from typical age-related degenerative changes, the specimens did not have any disease that could have affected the osteoligamentous structures. The specimens were mounted in resin at the occiput and most inferior vertebra (C5 or C6) with the occiput flexed 30° relative to the occipital mount and the inferior endplate of C5 or C6 parallel with its mount. This cervical spine posture with lordosis removed represents a straightened neck rather than normal lordotic posture.[17] The occiput and C5 or C6 vertebra were secured rigidly to custom aluminum fixtures within their mounts using screws. The aluminum fixture within the occipital mount had 4 rigidly attached bolts protruding superiorly for subsequent rigid attachment of the surrogate head. The mount for C5 or C6 and its aluminum fixture were designed for subsequent rigid attachment to a mass on a custom-built sled using a laterally aligned, double-ended threaded stud. I did not observe loosening at the mounting interfaces or mount failure during preliminary studies. Lightweight motion-tracking markers (model ASIN B000FMYIP6; SmallParts, Seattle, WA) were attached rigidly to each cervical vertebra and to both mounts.

A Hybrid III surrogate head (Humanetics Innovative Solutions, Plymouth, MI) was modified to include a 6-component load cell (MC3A force/torque sensor; Advanced Mechanical Technology, Inc, Watertown, MA) with an ultimate shear force of 3300 N, ultimate axial force of 6600 N, and ultimate sagittal moment of 165 Nm. The head (mass = 4.6 kg, sagittal moment of inertia = 0.0214 kg m^2) was attached rigidly to the occipital mount in anatomic location. The head had a motion-tracking marker rigidly fixed to its right side at its sagittal center-of-mass location. To provide postural head and neck stability and passive resistance to motion during head-first impact, the head and neck were stabilized using muscle-force replication, which was modified from a previous study.[18] The muscle-force replication was symmetric about the midsagittal plane and consisted of 2 anterior and 2 posterior cables originating from the head and anchored to preloaded springs with stiffness coefficients of 8.0 N/mm. The preload in each cable was 50 N, resulting in 200 N total compressive spinal preload immediately before impact. This preload was within the range of the estimated in vivo spinal compression computed using mathematical models: between 100 and 122 N in relaxed posture and 1164 and 1700 N with maximally active neck muscles.[19,20]

Head-First Impact and Monitoring

Each specimen was subjected to a single head-first impact with velocity at impact of 4.1 ± 0.3 m/s. The impact apparatus consisted of a mass rigidly fixed to the sled with the C5 or C6 mount of the specimen rigidly fixed at the front of the mass (Figure 1). The mass (55.5 kg) represented the equivalent torso mass of a heavier athlete or an obese male.[21] I assumed that the entire torso mass acted on the neck due to its forward momentum during head-first impact. An upward force was used to counterbalance the head weight and to maintain the head and neck posture before impact.

The sled was mounted on low-friction linear bearings, which translated along 2 precision-ground, stainless-steel shafts. Motion-tracking markers were fixed to the sled and

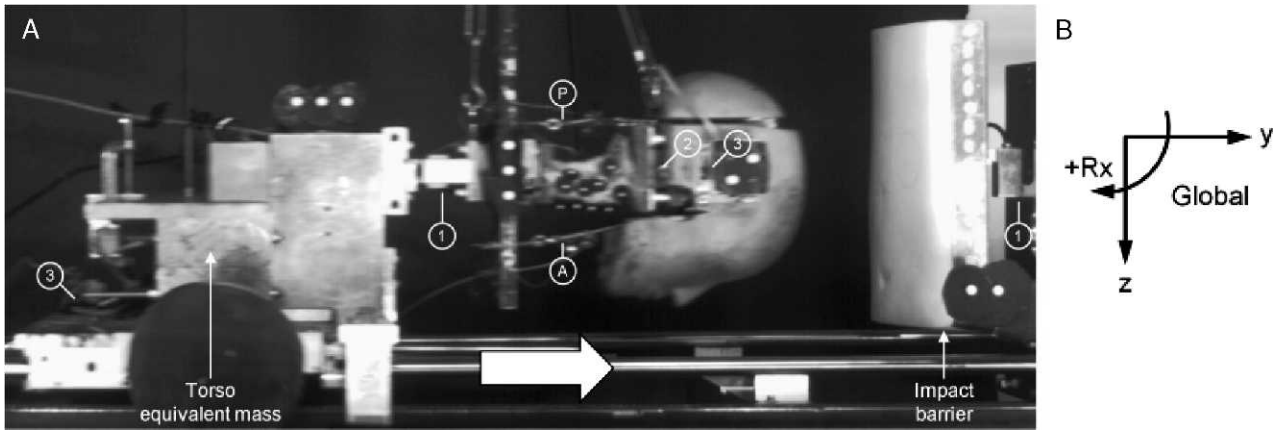

Figure 1. A, High-speed camera photograph of the head and neck specimen during simulated head-first impact. The model consisted of a human cadaveric cervical spine specimen mounted to a mass on the sled representing the equivalent torso mass and carrying an anthropometric surrogate head. The head and neck were stabilized using anterior (A) and posterior (P) muscle-force replication cables. Motion-tracking markers were rigidly fixed to the head, cervical vertebrae, sled, and impact barrier. Load cells included 1 component between the base of the neck and torso mass and at the impact barrier (1) and 6 components in the head (2). Biaxial accelerometers (3) are rigidly fixed to the head and torso mass. B, The global coordinate system was fixed to the ground and had its positive z axis oriented anteriorly, positive y axis oriented superiorly, and positive x axis oriented to the left relative to the specimen. Sagittal rotation was positive for flexion and negative for extension.

padded impact barrier. A high-speed potentiometer (model 3540S-1-203; Bourns, Riverside, CA) mounted to the sled was used to confirm sled translation computed using the flag marker data. The sled was accelerated using a custom-built acceleration generation system consisting of a piston, high-energy compression springs, and computer-controlled electromagnetic release. At the time of electromagnet release, a trigger signal initiated high-speed camera (MotionPRO; Redlake MSAD, San Diego, CA) recording. In preliminary studies, nonphysiologic neck motions and injuries were documented due to head impact and not due to the initial sled-acceleration phase. The padded barrier consisted of a pneumatic system (Original Line; Bimba, University Park, IL) that permitted adjustment of its energy absorption from rigid, no-energy absorption to gradual deformation. The padded barrier consisted of a 5-cm-thick, open-cell, highly deformable, polyurethane foam pad (density = 0.0288 g/cm^3, compressive strength = 3.8 kPa, tensile strength = 172 to 207 kPa) mounted to a rigid aluminum plate (model 325-4197; Enco, Fernley, NV). This foam pad provided head constraint and pocketing during head-first impact.

The impact apparatus was controlled fully by a personal computer and custom LabVIEW software (version 8.5; National Instruments, Austin, TX). Uniaxial load cells were used to measure impact barrier loads with an ultimate load of 10 kN (model LCCA-750; Omega Engineering, Inc, Stamford, CT) and loads at the base of the neck with an ultimate load of 40 kN (model LCCA-3K; Omega Engineering, Inc). Biaxial accelerations were measured at the head center of mass and C5 or C6 vertebra and had a capacity of 50*g* (model ADXL250JQC; Analog Devices, Norwood, MA). Load cell, accelerometer, and potentiometer data were sampled continuously at 1 kHz using an analog-to-digital converter and the LabVIEW program. The high-speed digital camera recorded the sagittal kinematics at 500 frames per second. Macroscopic neck injuries were determined by fluoroscopy and visual inspection after the impacts.

Data Analysis

Representative time-history responses were determined for intervertebral rotations and cervical spine curvature during head-first impact. *Neck buckling*, which was defined as rotation in opposing directions throughout the cervical spine, has been observed in previous head-first impact simulations of cadavers.[7] A *vertebral inflection point* was defined as the point above and below which the spinal levels rotated in opposing directions. The intervertebral rotations for the spinal levels above and below the inflection point were summed separately and normalized to the corresponding physiologic rotations obtained from intact flexibility tests. To visualize the cervical spine curvature, a phase diagram was created by plotting the normalized upper and middle cervical spine rotations.[22]

Specimen-specific kinetic and kinematic time-history responses during head-first impact were determined using the load cell and accelerometer data and analyses of the high-speed videos. Impact velocity was determined by numerical differentiation of the sled potentiometer data. The global coordinate system was fixed to the ground and had its positive z axis oriented anteriorly, positive y axis oriented superiorly, and positive x axis oriented to the left relative to the specimen (Figure 1). Loads included forces in lateral shear (Fx), tension and compression (Fy), and anteroposterior shear (Fz) and moments in flexion and extension (Mx), axial torque (My), and lateral torque (Mz). Loads were computed at the impact barrier (Fy), occipital condyles (6 components), and center of mass of the C5 or C6 vertebra (Fy). Mean ± standard deviation errors in the computed loads were 0.5 ± 1.8 N for shear force, –0.1 ± 2.2 N for axial force, and 0.7 ± 0.7 Nm for moment.[23] Accelerations were determined at the centers of mass of the head (Az and Ay) and C5 or C6 vertebra (Ay). Occipital condyle loads and head accelerations were expressed in the head coordinate system, which was fixed to and moved with the head. The global and head coordinate systems were aligned immediately before impact.

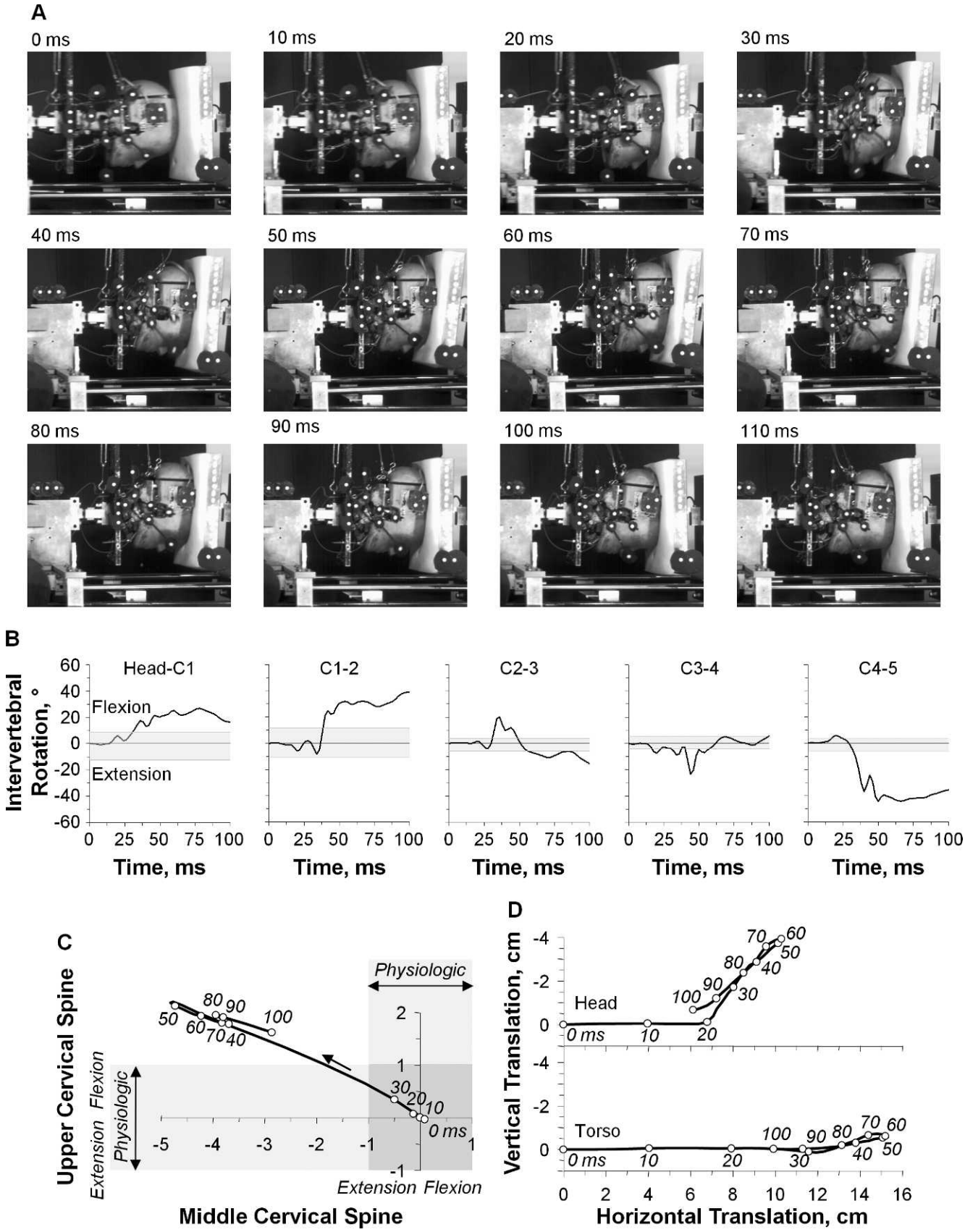

Figure 2. A representative example of head-first impact (specimen 2, peak barrier impact force = 6154.1 N). A, High-speed camera images are shown at time = 0 through 110 milliseconds in 10-millisecond increments. B, Time-history responses for intervertebral rotations. The physiologic rotation range, as determined from intact flexibility testing, is indicated by grey horizontal shading for each spinal level. C, Normalized upper and middle cervical spine rotation. The S-shape neck curvature is represented as the top left quadrant. The physiologic rotation bands for upper and middle cervical spine rotation are indicated with lightly shaded horizontal and vertical rectangles,

Custom MATLAB (The MathWorks, Inc, Natick, MA) programs automatically tracked the coordinates of all flag markers during the impacts and were used to compute head and torso motions. These motions consisted of translations, including axial separation and compression (Ty) and anteroposterior shear (Tz) and rotation (Rx), expressed in the global coordinate system. The mean ± standard deviation errors were –0.06° ± 0.17° for rotation[24] and 0.3 ± 0.2 mm for translation.[25]

All data were filtered digitally using a third-order, dual-pass, low-pass Butterworth filter with a cutoff frequency of 150 Hz. Average occurrence times of the first local and global compression force peaks at the impact barrier, occipital condyles, and C5 or C6 vertebra were compared using analysis of variance and post hoc Bonferonni pairwise tests. The α level was set at .05. I used Minitab 16 (Minitab, Inc, State College, PA) to analyze the data.

RESULTS

A representative example was chosen to illustrate the original high-speed movie images during head-first impact (Figure 2A). The high-speed movie images demonstrated dramatic neck compression, which was exemplified at 50 and 60 milliseconds. Head flexion remained within physiologic limits that was less than 10°. Excessive axial compression caused the cervical spine to buckle and fail. During buckling, nonphysiologic motions were observed in flexion at the upper cervical spine, head–C1, and C1–2 and extension at the subaxial spinal levels (Figure 2B). The phase diagram of normalized upper and middle cervical spine rotations included the physiologic rotation bands for the upper cervical spine and middle cervical spine (Figure 2C). The intersection of the 2 bands represents the physiologic rotation region. The areas outside this region represent potential injury zones due to nonphysiologic rotation. The C3 vertebra was identified as the inflection point for reversal of motion direction. The neck buckled in an S-shaped curvature, with the onset of nonphysiologic motion occurring first in extension at the middle cervical spine (32 milliseconds) and subsequently in flexion at the upper cervical spine (34 milliseconds). The time courses for head and C5 translations indicated that the onset of head and torso compression occurred at 10 milliseconds before the onset of intervertebral rotation (Figure 2D). The onset of posterior head translation commenced at 20 milliseconds. Head and torso rebound occurred simultaneously beginning at 56 milliseconds.

The specimen-specific time-history responses for loads, accelerations, and motions appear in Figure 3. No apparent lag time was observed among the onset of compression forces at the impact barrier, occipital condyles, and C5 or C6 vertebra, but the barrier and occipital condyle loads increased more rapidly than the C5 or C6 loads (Figure 3A and B). Predominant loads at the occipital condyles included compression coupled with anterior shear and flexion moment (Figure 3B and C). Average peak deceleration at the head was 27.9*g* at 17.6 milliseconds and at the C5 or C6 vertebra was 16.7*g* at 45.6 milliseconds (Figure 3D). The head accelerated posteriorly and then anteriorly (Figure 3E). Average peak motions of the head relative to the torso were 6.0 cm in compression at 56 milliseconds, 2.4 cm in posterior shear at 56 milliseconds, and 6.4° in flexion at 86 milliseconds (Figure 3F). The average deformation of the impact barrier pistons was 0.9 cm as measured after impact.

The first local compression force peaks at the impact barrier, occipital condyles, and C5 or C6 vertebra occurred earlier than all global compression peaks (F range = 9.1–157.5, $P < .001$; Table). The first local compression peaks reached a mean of 3070.0 ± 168.0 N at the impact barrier, 2868.1 ± 732.4 N at the occipital condyles, and 2884.6 ± 910.7 N at the C5 or C6 vertebra.

The fluoroscopic and visual inspections revealed severe macroscopic injuries, including occipital condyle fractures (specimens 1 and 5), atlas fractures (all specimens), type II (specimen 4) and type III (specimen 2) odontoid fractures, and subaxial comminuted burst and facet fractures (all specimens).

DISCUSSION

The present cadaveric head-neck model simulated horizontally aligned head-first impacts with a straightened neck, replicating traumatic neck compression during football, rugby, hockey, diving, wrestling, gymnastics, trampolining, and equestrian sports. Average peak neck compression force (7531.6 N) and velocity at impact (4.1 m/s) were consistent with the ranges computed for real-life head-first sports impacts that have caused cervical quadriplegia in athletes: 3611 to 8138 N for neck compression and 3.4 to 6.6 m/s for impact velocity (Table).[1,2] The impacts in this study caused clinically relevant compression fractures, including occipital condyle, atlas, odontoid, and subaxial comminuted burst and facet fractures. These results are consistent with those reported in previous clinical studies in which researchers[26–28] described multiple noncontiguous neck fractures due to traumatic head impacts.

The limitations of this model should be considered before interpreting these results. Given a lack of young cadaveric material, the sample size was limited to 5 specimens with an average age of 86.8 years, which was outside the age range of previous cadaveric studies (age range, 35–82 years).[7–10] The present specimens and the older specimens of the previous studies likely had decreased bone mass, density, and strength compared with the younger athletic population that sustains neck injuries due to head-first impacts. To determine occipital condyle loads, the model included a Hybrid III surrogate head modified to include a 6-component load cell rigidly attached to the occipital mount. I used a torso-equivalent rigid mass of 55.5 kg, which represented the mass of a heavier athlete or obese male.[21] I assumed that the entire torso mass acted on the neck due to its forward momentum during head-first impact. This represented the worst-case scenario for causation of neck injuries. In real-life head-first impacts,

←
respectively. Their intersection (darkly shaded) forms the physiologic region representing the safe curvature zone. The time course is indicated in 10-millisecond intervals. D, Head and torso translations in the global coordinate system with the time course are indicated in 10-millisecond intervals.

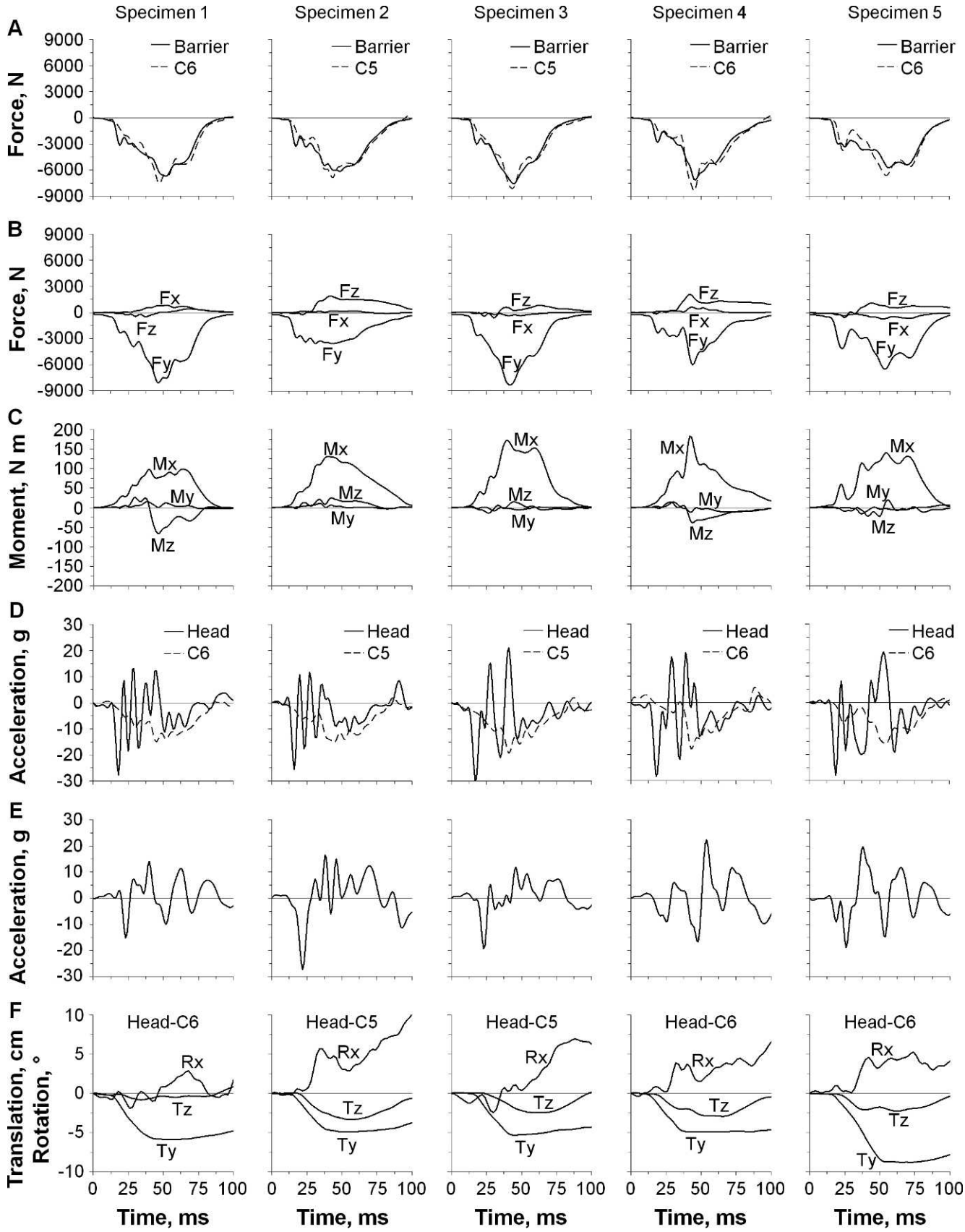

Figure 3. Specimen-specific time-history responses for loads, accelerations, and motions during head-first impact. A, The loads included impact forces at the barrier and C5 or C6 vertebra; B, forces at the occipital condyles including lateral shear (Fx), axial tension and compression (Fy), and anterior/posterior shear (Fz); and C, moments at the occipital condyles in flexion and extension (Mx), axial torque (My), and lateral torque (Mz). D, The accelerations included Ay for the head and C5 or C6; and E, Az for the head. F, The motions included translations (Ty and Tz) and sagittal rotation (Rx) for the head relative to the torso.

neck loading due to head impact and forward torso momentum is decoupled. The present cadaveric neck model did not include an active neuromuscular response; however, axial preload, postural head and neck stability, and passive resistance to motion were provided by muscle-force replication. The first local neck compression force peak occurred within 25 milliseconds on average, which was earlier than the active neuromuscular reflex (Table).[29] The importance of neck preload has been exemplified in previous studies, in which researchers[13] have shown that preload alters the dynamic head-neck responses during head-first impact. Although limited by factors associated with all cadaveric models, the present biomechanical model of head-first impact can be used to understand the mechanisms of neck injury and failure.

Previous vertical drop tests of human head-neck specimens in inverted postures have demonstrated a lag time between the onset of forces at the ground impact barrier and T1 vertebra.[7,9,10,30] The average lag time was 1.7 and 6.9 milliseconds for impacts into rigid and padded barriers, respectively, indicating a decoupled response of the head and neck. The apparent lack of lag time in the present horizontally aligned model can be attributed to several factors. The inverted posture of head-neck specimens with no axial preload in the previous vertical drop tests placed the neck in tension immediately before head impact, which might have accentuated the decoupled response.[7,9,10,30] This is in contrast to neck compression induced by muscle bracing in real-life head-first impacts. The compressive spinal preload of 200 N was nearly double that used in a previous study of a surrogate head-neck[13] but less than that produced with maximally active neck muscles. The present specimens were from older donors, and their cervical discs were degenerated, which might have contributed to the lack of decoupled head and neck response. Whereas I did not observe lag time, I did observe a more rapid initial increase in occipital condyle loads compared with C5 or C6 loads (Figure 3A and B), with the first local compression peak occurring initially at the occipital condyles (19.6 milliseconds) and subsequently at the C5 or C6 vertebra (25.0 milliseconds; Table). In a recent study of vertical drop tests of a surrogate head-neck, researchers[13] demonstrated a reduction in lag time from 6.2 milliseconds with no preload to 2.2 milliseconds with 104 N of preload. This decrease in lag time with increasing axial preload indicates that muscle bracing by athletes in anticipation of head-first impact, which can exceed 1000 N,[19] might minimize the lag time.

In the previous cadaveric studies, investigators have defined the onset of bony injury as the first decrease in axial neck load with increasing spinal deformation. In their series, Nightingale et al[7] observed an average compressive neck load of 1727 N at the onset of bony injury, occurring from 14 to 19 milliseconds for impacts into a padded ground barrier. The present model demonstrated that the first local peak in compression force occurred at the occipital condyles at 19.6 milliseconds and at the C5 or C6 vertebra at 25.0 milliseconds (Table). These transient decreases in compression force occurred with increasing axial compressive deformation, ranging from 0.9 to 2.4 cm. These results suggest that the onset of the observed fractures of the occipital condyles and upper cervical vertebrae might have occurred before the onset of fractures

Table. Occurrence Times of the First Local and Global Compression Force Peaks at the Impact Barrier, Occipital Condyles, and C5 or C6 Vertebra Ordered Chronologically (Mean ± SD)[a]

Event	Time, ms	Compression Force, N			Flexion Moment, Nm	Head Motion Relative to Torso		
		Impact Barrier	Occipital Condyles	C5 or C6	Occipital Condyles	Flexion, °	Posterior Shear, cm	Compression, cm
First local compression force peak								
Impact barrier	18.8 ± 1.5	3070.0 ± 168.0	2744.3 ± 518.1	1511.6 ± 360.0	30.0 ± 12.3	0.3 ± 0.6	0.1 ± 0.1	0.9 ± 0.5
Occipital condyles	19.6 ± 2.1	2959.9 ± 95.9	2868.1 ± 732.4	1943.5 ± 910.4	33.6 ± 15.6	0.2 ± 0.6	0.1 ± 0.1	1.1 ± 0.6
C5 or C6	25.0 ± 3.7	2950.4 ± 562.5	3287.7 ± 891.9	2884.6 ± 910.7	45.6 ± 13.0	0.1 ± 0.7	0.6 ± 0.3	2.4 ± 1.1
Global compression force peak								
Occipital condyles	45.8 ± 4.8	6225.3 ± 747.0	6485.9 ± 1925.5	7391.6 ± 677.1	135.6 ± 37.2	2.3 ± 2.1	1.8 ± 0.9	5.9 ± 1.7
C5 or C6	46.6 ± 5.0	6464.0 ± 782.1	6414.6 ± 1918.9	7531.6 ± 757.1	131.1 ± 32.0	2.4 ± 2.0	1.8 ± 0.9	5.9 ± 1.6
Impact barrier	49.4 ± 5.2	6662.6 ± 742.0	6057.8 ± 1874.0	6929.0 ± 1153.8	124.6 ± 24.8	2.3 ± 1.6	2.0 ± 1.0	6.0 ± 1.6

[a] Average data at each event time are provided for: compression force at the barrier, occipital condyles, and C5 or C6; flexion moment at the occipital condyles; and head motions relative to the torso including flexion, posterior shear, and compression.

at the inferior vertebrae due to abrupt deceleration of the head as loads were transferred inferiorly through the neck. The onset of the observed fractures of the inferior vertebrae were likely due to continued forward torso momentum that transferred loads superiorly through the neck, which likely exacerbated the injuries to the occipital condyles and upper cervical vertebrae. The magnitudes of the first local peaks in compression force were 2868.1 ± 732.4 N at the occipital condyles and 2884.6 ± 910.7 N at the C5 or C6 vertebra (Table), both of which were higher than the 1727 N local compression peak reported by Nightingale et al.[7] This difference might be due in part to the higher impact velocity used in the present study (4.1 m/s) than in the study by Nightingale et al[7] (3.2 m/s).

In the previous biomechanical studies, neck injuries due to head-first impact were attributed to abrupt stoppage and rebound of the head combined with continued torso momentum.[7,9,10,30] Between 38% and 54% of total neck compression force was attributed to head rebound.[7] In these previous studies, head-neck specimens were dropped vertically onto a nondeformable steel plate with and without a padded surface. Head-first sport impacts most often involve the head striking a padded, deformable surface, which might reduce or negate head rebound. These surfaces include the padding and soft tissues of an opponent, compressive playing surfaces, hockey rink boards, and goal posts.[16] Helmeted impacts increase the energy absorption due to padding within the helmet. I replicated these injury scenarios by incorporating a padded, pneumatic impact barrier, which deformed 0.9 cm on average during the impacts. The barrier also allowed angular deformation, as demonstrated in the representative high-speed movie images (Figure 2A, times 30–80 ms). This caused posterior head translation (Figures 2D and 3F) and might have accentuated the S-shape neck curvature (Figure 2C). I observed continued forward motion of the head after the onset of injury. The onset of head rebound occurred simultaneously at 56 milliseconds at the time of peak head and torso motions in axial compression and posterior shear (Figure 2D). Neck injuries due to excessive axial compression loads in this model were caused by abrupt deceleration of the head and continued forward torso momentum before simultaneous rebound of the head and torso.

The present results are consistent with those reported in previous studies in which investigators noted neck compression injuries within 20 milliseconds of impact before substantial head rotation.[7,9] Nightingale et al[10] observed that a large amount of head rotation might protect the neck from injury by allowing it to escape the path of the oncoming torso. The present results indicated that head rotation consistently remained within physiologic limits ($<10°$) and average peak head posterior translation was 2.4 cm (Figure 3F). These data showed that head motions were of insufficient magnitude to allow the head and neck to escape the path of the oncoming torso. In contrast, average peak axial compression reached 6.0 cm with an average onset at 10 milliseconds. This compression is greater than the 2.5- to 3.5-cm compression observed with vertical impacts of unrestrained cadavers in inverted postures, during which the head flexed abruptly, causing chin-to-chest contact and allowing the head and neck to partially escape the path of the oncoming torso.[8] These cumulative findings suggest that axial compression load and neck compressive deformation are the predominant mechanisms that cause early injuries during head-first impact, whereas subsequent injurious neck buckling causes nonphysiologic intervertebral motions with minimal head rotation.

CONCLUSIONS

The present study determined the head and neck biomechanical responses and neck failure mechanisms using a cadaveric cervical spine model in simulated head-first impacts. The first local compression force peaks at the impact barrier, occipital condyles, and neck occurred earlier than all global compression peaks. Head rotation remained within physiologic limits. Neck injuries due to excessive axial compression occurred within 20 milliseconds of impact and were caused by abrupt deceleration of the head and continued forward torso momentum before simultaneous rebound of the head and torso. Continued biomechanical and epidemiologic studies of neck injuries and injury mechanisms due to head-first impact ultimately will lead to reduced frequency and severity of sports-induced neck trauma.

ACKNOWLEDGMENTS

This research was supported by grant 5R01CE001257 from the Centers for Disease Control and Prevention, Atlanta, Georgia.

REFERENCES

1. Torg JS, Vegso JJ, O'Neill MJ, Sennett B. The epidemiologic, pathologic, biomechanical, and cinematographic analysis of football-induced cervical spine trauma. *Am J Sports Med*. 1990;18(1):50–57.
2. Torg JS. *Athletic Injuries to the Head, Neck, and Face*. 2nd ed. St Louis, MO: Mosby-Year Book, Inc; 1991.
3. Goldberg W, Mueller C, Panacek E, et al. Distribution and patterns of blunt traumatic cervical spine injury. *Ann Emerg Med*. 2001;38(1):17–21.
4. DeVivo MJ, Krause JS, Lammertse DP. Recent trends in mortality and causes of death among persons with spinal cord injury. *Arch Phys Med Rehabil*. 1999;80(11):1411–1419.
5. National Spinal Cord Injury Statistical Center. Spinal cord injury facts and figures at a glance. https://www.nscisc.uab.edu/PublicDocuments/nscisc_home/pdf/Facts%202011%20Feb%20Final.pdf. Published February 2011. Accessed March 1, 2012.
6. Drakos MC, Feeley BT, Barnes R, Muller M, Burruss TP, Warren RF. Lower cervical posterior element fractures in the National Football League: a report of two cases and a review of the literature. *Neurosurgery*. 2011;68(6):E1743–E1749.
7. Nightingale RW, McElhaney JH, Richardson WJ, Myers BS. Dynamic responses of the head and cervical spine to axial impact loading. *J Biomech*. 1996;29(3):307–318.
8. Yoganandan N, Sances A Jr, Maiman DJ, Myklebust JB, Pech P, Larson SJ. Experimental spinal injuries with vertical impact. *Spine*. 1986;11(9):855–860.
9. Nightingale RW, McElhaney JH, Richardson WJ, Best TM, Myers BS. Experimental impact injury to the cervical spine: relating motion of the head and the mechanism of injury. *J Bone Joint Surg Am*. 1996;78(3):412–421.
10. Nightingale RW, Richardson WJ, Myers BS. The effects of padded surfaces on the risk for cervical spine injury. *Spine (Phila Pa 1976)*. 1997;22(20):2380–2387.
11. Cusick JF, Yoganandan N, Pintar F, Gardon M. Cervical spine injuries from high-velocity forces: a pathoanatomic and radiologic study. *J Spinal Disord*. 1996;9(1):1–7.
12. Pintar FA, Yoganandan N, Voo L, Cusick JF, Maiman DJ, Sances A. Dynamic characteristics of the human cervical spine. *Society of*

Automotive Engineers Technical Paper 952722. 1995. doi:10.4271/952722.
13. Nelson TS, Cripton PA. A new biofidelic sagittal plane surrogate neck for head-first impacts. *Traffic Inj Prev*. 2010;11(3):309–319.
14. Nightingale RW, Camacho DL, Armstrong AJ, Robinette JJ, Myers BS. Inertial properties and loading rates affect buckling modes and injury mechanisms in the cervical spine. *J Biomech*. 2000;33(2):191–197.
15. Camacho DL, Nightingale RW, Myers BS. The influence of surface padding properties on head and neck injury risk. *J Biomech Eng*. 2001;123(5):432–439.
16. Swartz EE, Floyd RT, Cendoma M. Cervical spine functional anatomy and the biomechanics of injury due to compressive loading. *J Athl Train*. 2005;40(3):155–161.
17. Descarreaux M, Blouin JS, Teasdale N. A non-invasive technique for measurement of cervical vertebral angle: report of a preliminary study. *Eur Spine J*. 2003;12(3):314–319.
18. Ivancic PC, Panjabi MM, Ito S, Cripton PA, Wang JL. Biofidelic whole cervical spine model with muscle force replication for whiplash simulation. *Eur Spine J*. 2005;14(4):346–355.
19. Moroney SP, Schultz AB, Miller JA. Analysis and measurement of neck loads. *J Orthop Res*. 1988;6(5):713–720.
20. Chancey VC, Nightingale RW, Van Ee CA, Knaub KE, Myers BS. Improved estimation of human neck tensile tolerance: reducing the range of reported tolerance using anthropometrically correct muscles and optimized physiologic initial conditions. *Stapp Car Crash J*. 2003;47:135–153.
21. Chambers AJ, Sukits AL, McCrory JL, Cham R. The effect of obesity and gender on body segment parameters in older adults. *Clin Biomech (Bristol, Avon)*. 2010;25(2):131–136.
22. Ivancic PC, Xiao M. Cervical spine curvature during simulated rear crashes with energy-absorbing seat. *Spine J*. 2011;11(3):224–233.
23. Ivancic PC, Panjabi MM, Ito S. Cervical spine loads and intervertebral motions during whiplash. *Traffic Inj Prev*. 2006;7(4):389–399.
24. Ivancic PC, Wang JL, Panjabi MM. Calculation of dynamic spinal ligament deformation. *Traffic Inj Prev*. 2006;7(1):81–87.
25. Pearson AM, Ivancic PC, Ito S, Panjabi MM. Facet joint kinematics and injury mechanisms during simulated whiplash. *Spine (Phila Pa 1976)*. 2004;29(4):390–397.
26. Sharma OP, Oswanski MF, Yazdi JS, Jindal S, Taylor M. Assessment for additional spinal trauma in patients with cervical spine injury. *Am Surg*. 2007;73(1):70–74.
27. Barrett TW, Mower WR, Zucker MI, Hoffman JR. Injuries missed by limited computed tomographic imaging of patients with cervical spine injuries. *Ann Emerg Med*. 2006;47(2):129–133.
28. Miller CP, Brubacher JW, Biswas D, Lawrence BD, Whang PG, Grauer JN. The incidence of noncontiguous spinal fractures and other traumatic injuries associated with cervical spine fractures: a 10-year experience at an academic medical center. *Spine (Phila Pa 1976)*. 2011;36(19):1532–1540.
29. Foust DR, Chaffin DB, Snyder RG, Baum JK. Cervical range of motion and dynamic response and strength of cervical muscles. *Society of Automotive Engineers Technical Paper 730975*. 1973. doi:10.4271/73975.
30. Nightingale RW, McElhaney JH, Camacho DL, Kleinberger M, Winkelstein BA, Myers BS. The dynamic responses of the cervical spine: buckling, end conditions, and tolerance in compressive impacts. *Society of Automotive Engineers Technical Paper 973344*. 1997. doi:10.4271/973344.

Address correspondence to Paul C. Ivancic, PhD, Department of Orthopaedics and Rehabilitation, Yale University School of Medicine, 333 Cedar Street, PO Box 208071, New Haven, CT 06520-8071. Address e-mail to paul.ivancic@yale.edu.